

Journal of Biomedical Optics

SPIEDigitalLibrary.org/jbo

On the birefringence of healthy and malaria-infected red blood cells

Aditya K. Dharmadhikari
Himanish Basu
Jayashree A. Dharmadhikari
Shobhona Sharma
Deepak Mathur



SPIE

On the birefringence of healthy and malaria-infected red blood cells

Aditya K. Dharmadhikari,^a Himanish Basu,^a Jayashree A. Dharmadhikari,^b Shobhona Sharma,^a and Deepak Mathur^{a,b}

^aTata Institute of Fundamental Research, 1 Homi Bhabha Road, Mumbai 400 005, India

^bManipal University, Centre for Atomic and Molecular Physics, Manipal 576 104, India

Abstract. The birefringence of a red blood cell (RBC) is quantitatively monitored as it becomes infected by a malarial parasite. Large changes occur in the cell's refractive index at different stages of malarial infection. The observed rotation of an optically trapped, malaria-infected RBC is not a simple function of shape distortion: the malarial parasite is found to itself exercise a profound influence on the rotational dynamics by inducing stage-specific birefringence. Our measurements shed new light on the competition between shape- and form-birefringence in RBCs. We demonstrate the possibility of using birefringence to establish very early stages of infected parasites and of assessing various factors that contribute to birefringence in normal and infected cells. Our results have implications for the development and use of noninvasive techniques of quantifying changes in cell properties induced by malaria disease pathology. © The Authors. Published by SPIE under a Creative Commons Attribution 3.0 Unported License. Distribution or reproduction of this work in whole or in part requires full attribution of the original publication, including its DOI. [DOI: [10.1117/1.JBO.18.12.125001](https://doi.org/10.1117/1.JBO.18.12.125001)]

Keywords: red blood cells; malaria; birefringence; optical trapping; optical properties; tweezers.

Paper 130509R received Jul. 19, 2013; revised manuscript received Sep. 20, 2013; accepted for publication Oct. 30, 2013; published online Dec. 2, 2013.

1 Introduction

The importance of blood has been known to humankind since ancient Indian texts on internal medicine were written around 300 BCE (Ref. 1), and, subsequently, the human circulatory system was described by the Egyptian surgeon Ibn An-Nafis^{2,3} in the 13th century. It was established that mature red blood cells (RBCs) are specialized for their primary function of oxygen delivery after traversing a network of blood vessels and capillaries.⁴ Such RBCs are differentiated to the extent that they possess no nucleus or protein-synthesizing machinery and are, therefore, refractory to most infective disease agents. Malaria is one among the parasitic diseases that develop in RBCs, with the *Plasmodium falciparum* variant being the most pathological. It causes cerebral malaria, precipitating from increased rigidity of infected RBCs and resulting in the blockage of blood flow in microcapillaries that curtails blood supply to the brain and other organs. Understanding parasite-induced changes in RBCs is imperative toward the control of pathology.

Capturing disease states has relied on visualization of RBCs, with optical physics playing a major role since the 17th century through the invention of microscopes. The malaria disease was discovered by visualizing infected RBCs in 1884.⁵ Contemporary development of optical tools,⁶ like phase contrast and topographic phase microscopies,^{7,8} have opened newer vistas for studies of cellular biomechanics. It has been known for more than half a century that healthy human RBCs exhibit intrinsic birefringence that arises from hemoglobin^{9,10} and the cell membrane.¹¹ Upon infection by a malarial parasite, the cell's hemoglobin content undergoes changes that affect birefringence: as the parasite grows (over 48 h), it crystallizes

hemoglobin into hemozoin.^{12,13} Hemozoin crystals are highly birefringent and they, thus, offer opportunities for studying malaria-infected RBCs through polarization microscopy.¹³

Using polarized light microscopy, a method for localizing intracellular pigmented malaria parasites has been demonstrated in wet prepared blood samples at very low (0.01%) parasitemia.¹⁴ Depolarization of laser light has also been analyzed for diagnosing malarial infections.¹⁵ Recently, tomographic phase microscopy⁷ has been utilized to map the stage-specific, three-dimensional refractive index distribution in malaria-infected RBCs.¹⁶ They have shown regions of low refractive index (location of vacuole of parasite) and high refractive index (location of hemozoin). This represents the only study so far on stage-specific malarial infections of RBCs. However, we note that infection of an RBC by *P. falciparum* also results in significant shape alterations that contribute to changes in birefringence. It would clearly be of considerable interest to conduct studies that can differentiate between shape-induced and intrinsic birefringence.

In recent years, there has been significant work that has utilized an optical trap^{17,18} for studying mechanical, viscoelastic, and osmolarity-induced changes of single RBCs.^{6,19-21} Upon placing a birefringent material in an optical trap, rotation is induced such that the laser light passes through the more polarizable axis.^{22,23} Our earlier experiments²⁴ have established that malaria-infected RBCs undergo shape distortion and rotational motion upon their interaction with a tightly focused laser beam of the type that is encountered within an optical trap; the normal RBCs do not rotate but align themselves along the direction of laser electric field. The distortion of shape has been characterized in terms of Euler buckling;²⁵ it plays an important role in the rotational motion by enhancing the spatial anisotropy of the cell's polarizability tensor, α , such that the $(\alpha \cdot E)$ interaction with the optical field gives rise to a torque that, in turn, causes rotation of the trapped RBC (E denotes the amplitude of the

Address all correspondence to: Deepak Mathur, Tata Institute of Fundamental Research, 1 Homi Bhabha Road, Mumbai 400 005, India. Tel: +91 22 2278 2736; Fax: +91 22 2280 4611; E-mail: atmol1@tifr.res.in

laser's optical field). The torque results from unbalanced optical forces acting on different sides of the trapped cell. Rotations due to such shape anisotropy are expected to be similar to those of RBCs that have undergone hyperosmotic shock²⁶ (osmotic shock also induces shape changes)—they scale with laser power. Such rotations have been experimentally characterized by combining optical trap technology with fluorescence and liquid flow methods,²⁶ but a proper insight into the physics that drives the dynamics remains elusive. Moreover, rotations are also known to be caused in optically trapped objects that may be isotropic in shape but are optically anisotropic, as in birefringent materials that possess two axes of polarization, with one axis being more polarized than the other.

Here, we describe utilization of an optical trap to quantitatively monitor the influence that a malarial parasite has on optical properties of RBCs; specifically, we probe parasite-induced linear birefringence (retardance). By quantifying birefringence in uninfected but shape-distorted cells, as well as in parasitized cells, we distinguish form- and intrinsic-birefringence at different stages of parasite infection. The former depends on cell shape, while the latter reflects the state of hemoglobin in the infected RBC. We also quantify changes in the refractive index of normal and infected RBCs by analyzing the polarization of light transmitted through single, optically trapped cells; the refractive index more than doubles at later stages of malarial infection. Our systematic experiments on how matter affects light were conducted on live single cells maintained under physiological conditions; our findings have implications for the use of noninvasive, real-time methods for quantifying changes in cell properties induced by pathological states that accompany malaria. The information forthcoming from our trap-based experiments may stimulate theoretical and computational efforts that have a bearing on parameters contributing to general hematological disorders.

2 Experimental Method

Our optical trap (see Ref. 27 and references therein) consists (see Fig. 1) of a continuous wave diode pumped Nd:YVO₄ laser operating at 1064 nm with maximum power of 1.0 W. The initial beam, of 2 mm diameter, is passed through a Glan-laser polarizer (P) (extinction ratio 10⁻⁵:1) and half-wave plate (HWP). It is then expanded to 8 mm diameter (using lenses L1 and L2) and is routed through mirrors M1 and M2 on to a 1:1 telescope (lenses L3 and L4). Using mirrors M3 to M5, the beam is then transported to a 100× microscope objective (Nikon) with numerical aperture (NA) of 1.3 and is focused on a glass coverslip on which the sample (S) is placed. We measured laser power after the objective using a calibrated silicon photodiode coupled to an integrating sphere. The sample on the coverslip was imaged using mirror M6 and a CCD camera. A tungsten halogen lamp was used along with a condenser to illuminate the sample.

The laser light transmitted through the sample (in this experiment, a live RBC) was collected by a high-NA water-immersed condenser (Nikon WI 0.9) and routed through a turning mirror M7. The light was then loosely focused (by lens L5) and passed through a Glan-laser analyzer (A). The photodiode (PD) detected the intensity of analyzed light leaking from the crossed analyzer. The PD signal was measured using a digital storage oscilloscope and stored on a computer. As described in earlier work,²⁶ asexual stages of *Plasmodium falciparum* 3D7 strain were maintained *in vitro* at 5% hematocrit in RPMI 1640

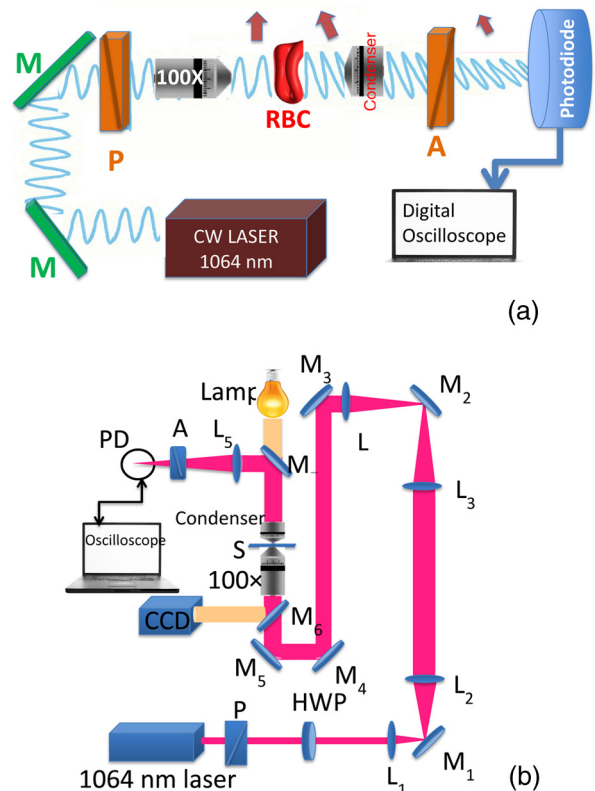


Fig. 1 (a) Schematic representation of how the plane polarized light is retarded after passing through a birefringent material [like a red blood cell (RBC)]. The transmitted light is analyzed by analyzer A and is collected on a photodiode. (b) Our optical trap setup including a half-wave plate polarizer (HWP) and analyzer (A). The leaked light is collected by a photodiode connected to an oscilloscope.

medium having 0.5% albumax and 10 $\mu\text{g/ml}$ gentamycin sulphate in a humidified chamber containing 5% CO₂ at 37°C in human erythrocytes of serological type B+.²⁸ In order to obtain synchronized cultures, the parasites were treated with sorbitol.²⁹ Briefly, *P. falciparum* cultures, which have >2 to 3% ring-stage parasite-infected RBCs, were incubated in 5% sorbitol (w/v) made in double-distilled water for 15 min at 37°C. The cells were then pelleted at 3,000 rpm for 6 min, washed twice with incomplete RPMI, and subsequently resuspended in complete RPMI (i.e., with albumax) at 50% hematocrit. Fresh RBCs (also 50% hematocrit) were added to the synchronized culture (in 1:1 ratio) and were then cultured at 5% hematocrit (as described above). The *P. berghei* ANKA and *P. yoelli* strains were maintained by passaging asexual stages through BALB/c mice. Tail bleeds were collected from mice showing ~20 to 40% peripheral blood parasitemia, and diluted 1:10 in incomplete RPMI. About 100 μl of this dilution was injected intraperitoneally into naïve BALB/c mice for the expansion of parasites. Parasitemia was monitored by microscopic examination of blood smears stained with Giemsa. Blood samples from humans and mice were collected in a sterile tube containing the anticoagulant ACD (136 mM glucose; 38 mM citric acid monohydrate and 75 mM sodium citrate) and centrifuged at 3,000 rpm for 10 min for separating the RBCs and plasma. The plasma and buffy coat containing white blood cells were aspirated out and purified erythrocytes were washed with sterile RPMI (Life Technologies Inc.) medium with 28 mM NaHCO₃,

25 mM HEPES, and 10 $\mu\text{g}/\text{ml}$ gentamycin sulphate. The erythrocytes were resuspended in sterile RPMI medium containing 0.5% albumax (Life Technologies Inc.) as a 50% v/v suspension, and diluted for use.

For osmolarity-perturbed human RBCs, 100 μl of blood was drawn from a finger prick into a vial containing 0.9 mg of anticoagulant powder (where each gram of anticoagulant comprised 450 mg of dextrose, 400 mg of sodium citrate, and 150 mg of citric acid). The addition of such an anticoagulant does not change the physical parameters (such as volume or viscosity) of the blood as a whole nor of the RBCs.³⁰ The blood was then centrifuged at 600 g for 5 min. The supernatant containing most of the serum proteins was discarded, while the pellet was resuspended in isotonic (300 mOsm) phosphate-buffered saline (PBS). This process was repeated at least five times to ensure maximal removal of serum proteins. After the last centrifugation process, the volume of the pellet was measured and an equal amount of PBS was added to the pellet to achieve 50% hematocrit. For creating different osmolalities, 10 \times PBS solutions were diluted with double-distilled water. Cells were then incubated in different osmolarity-perturbed solutions for 30 min before use in the experiment.

All our experiments were conducted in accordance with rules and procedures approved by the Tata Institute of Fundamental Research Human and Animal Ethics Committee. Blood samples were obtained from a volunteer after obtaining written, informed consent.

Typically RBCs (either malaria infected or osmolarity perturbed) were introduced into our optical trap by placing ~ 10 to 20 μl of cell suspension on a coverslip placed on a translation stage. Upon moving a single RBC toward the trap focus, it folded into a rod shape and rotated under the influence of the trap, as described in the literature.^{19,24} To study the birefringent properties of RBCs, the rotating cell was placed between a polarizer and analyzer whose planes were crossed. The light transmitted through the RBC was collected by our water-immersed condenser and routed through a turning mirror M7. The light was then loosely focused ($f = 25$ cm) and passed through a Glan-laser analyzer. A PD detected the intensity of analyzed light that leaked from the crossed polarizer-analyzer as the RBC rotated between them. We repeated such measurements at different power levels.

We determined the retardation by monitoring the light leaked by our polarizer-analyzer combination. We note that retardation is due to the phase change that is introduced by any birefringent material in two polarization states. In order to quantify the retardation, we first carried out a calibration procedure by rotating an HWP in between the polarizer-analyzer combination without any RBC. An HWP was rotated (through specific angles) and the leaked light was recorded using a PD. A plot of light intensity (as quantified by PD voltage) against HWP angle allowed us to estimate the retardation introduced by the RBC in terms of PD voltage. With no RBC present, the light emerging out of the analyzer was negligibly small, as its plane was crossed with the polarizer's plane. However, the presence of an RBC ensured sufficient retardation of light after it passed through the analyzer, and this change was found to depend on the polarization angle of the incident light as well as the angle of the rod-like RBC (Fig. 2). As the cell rotated, this angle continuously changed, with maximum retardance occurring when the angle between the RBC's axis and the incident light was 45 deg

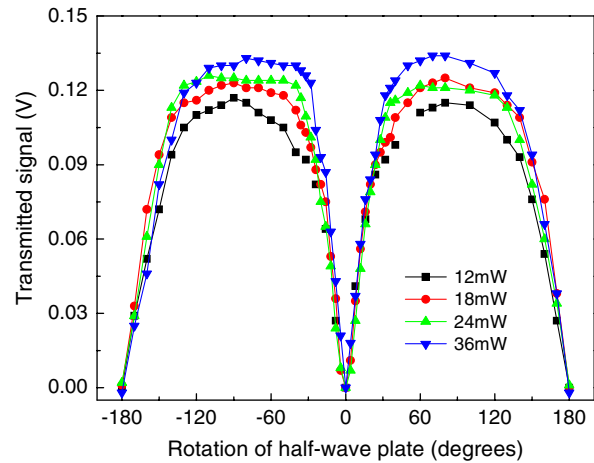


Fig. 2 Voltage generated by the photodiode due to light leakage in between a crossed-polarizer and analyzer, when the plane of polarization of the light after the polarizer is changed by means of a half-wave plate (see text). The vertical axis was measured with a least count of 2 mV and the error along the horizontal axis was ± 0.5 deg.

(Fig. 3). The value at the maxima observed under such circumstances is a measure of the RBC's birefringence.

3 Results and Discussion

Before presenting the details of our results, it is instructive to outline our experimental procedure with reference to Fig. 1(a), which is a schematic illustration of how a birefringent material introduces retardation. To probe RBC birefringence we utilized the setup shown in Fig. 1(b) by quantifying retardance induced by birefringence: for any rotational motion of an RBC trapped in cross-polarized light, the photodiode voltage is a direct measure of the retardance angle of the polarized light as it passes through the birefringent RBC. This angle is related to refractive index change, as shown in Fig. 3. Occurrence of two peaks when the analyzer is crossed in a single rotation cycle is clear-cut indication of the trapped RBC's birefringence [Fig. 3(a)]. When the analyzer was parallel, we observed only a single peak, indicating a chopper-like behavior of the RBC [Fig. 3(b)]. We made measurements on two types of shape-distorted RBCs: those whose shapes are distorted simply by changing osmolarity and those with malaria parasite-induced shape distortions. As already noted, there are two types of anisotropies: those related to shape changes give rise to form-birefringence, while those that are induced by biochemical alterations within the cell account for intrinsic birefringence.

Our experimentally measured intensity variations contain information on the RBC birefringence properties. However, quantification of such birefringence would require use of a general, all-encompassing model. In the case of RBCs, it is not possible to rule out the role played by polarizing-depolarizing interactions, like scattering-induced diattenuation and depolarization. Specifically, a model based on electromagnetic theory, which properly incorporates the effect of the RBC's scattering and polarization properties, would be required to simulate the variations of transmitted light detected in our experiments. Such simulation would then allow extraction of the birefringence properties of the RBCs in a quantitative fashion. Such a theoretical endeavor is formidable and well beyond the scope of the present studies. However, a simplistic approach is possible to help rationalize the observations we report

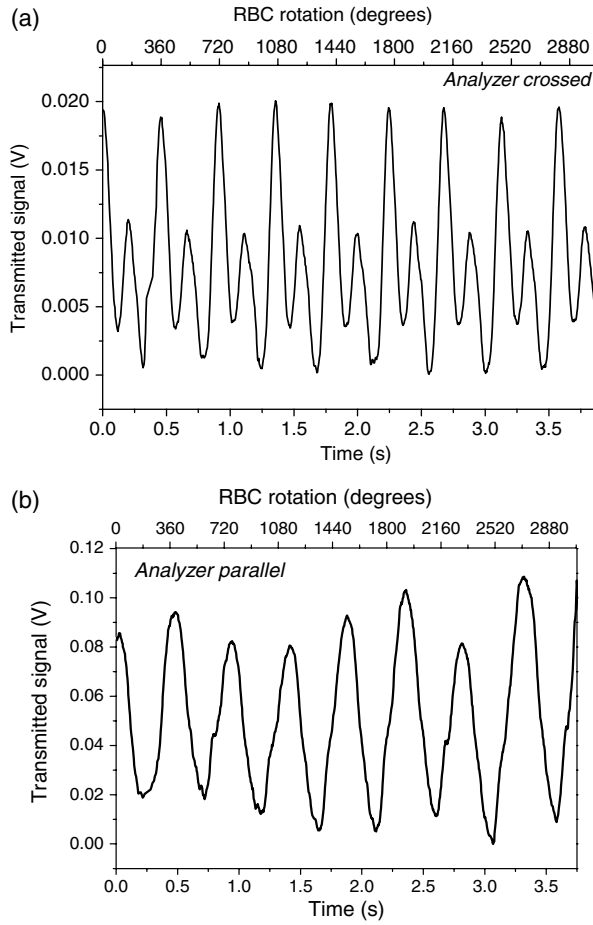


Fig. 3 Transmitted light intensity when a single, trapped RBC rotates, as recorded on a photodiode when the analyzer is crossed with the polarizer (a) and when the analyzer has its plane parallel to the polarizer (b).

here. So, we assume that linear birefringence is the dominant effect in RBCs, and we estimate the trend in variation of birefringence of optically trapped, malaria stage-dependent, infected RBCs as well as for RBCs that were not malaria infected but whose shape was perturbed by altering osmolarity. In case of osmolarity-induced shape-distorted RBCs, the resulting form-birefringence induces the cell to rotate within our trap, as indicated in Fig. 4, which also shows rotations due to the intrinsic birefringence of malaria-infected cells. In the former case, we made measurements on cells using osmolarities ranging from 150 to 1200 oSm; the rotational behavior did not depend on osmolarity change, with the peak-to-peak photodiode voltage remaining at 20 mV. The retardance (measured in degrees) measured for 20 mV change in photodiode voltage corresponds to 6 deg, which, in conjunction with the relation³¹

$$2\Delta\theta = \Delta n L 2\pi / \lambda, \quad (1)$$

yields a value of $\Delta n = 1.2 \times 10^{-2}$ for $L = 3 \mu\text{m}$ and wavelength $\lambda = 1064 \text{ nm}$. Here, Δn is the refractive index change. In the case of malaria-infected cells, we found that the PD voltage depended on infection stage. Our measurements were made on a synchronous culture of the malarial parasite at fixed time points. In all results that we present in the following, each data point represents an average of measurements made on 25 RBCs. Data obtained after 5 and 11 h of infection (Fig. 4) clearly show

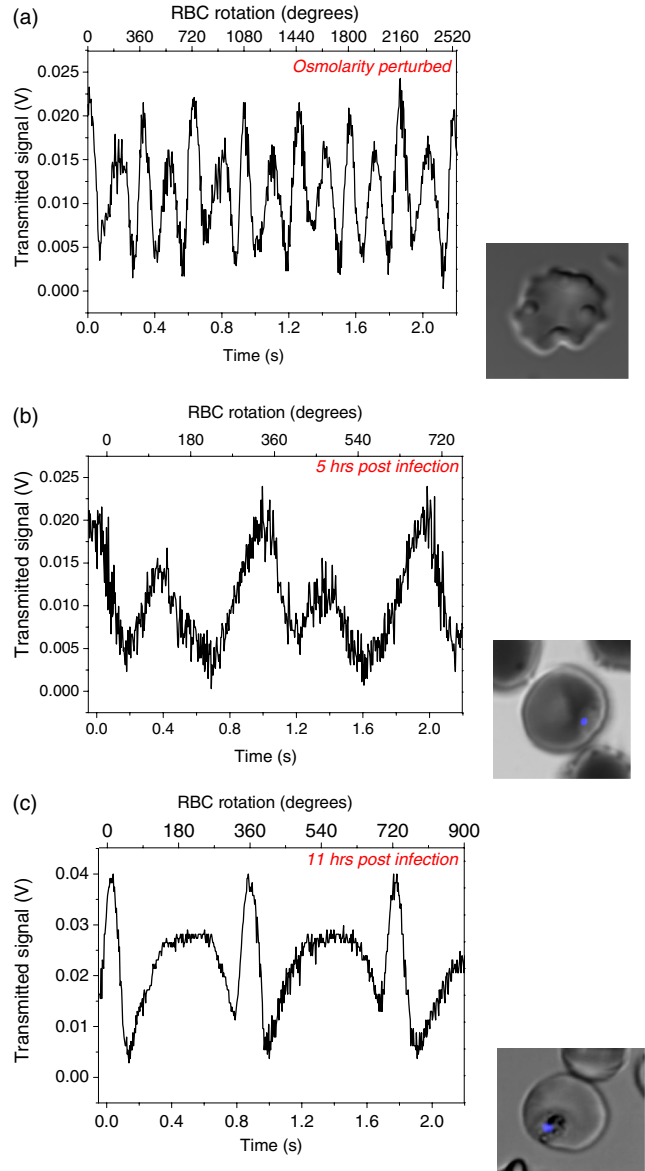


Fig. 4 Transmitted light intensity when a trapped RBC rotates, as recorded using a photodiode for osmolarity perturbed cells (a), malaria-infected cells, 5 h postinfection (b), and malarial-infected cells, 11 h postinfection (c). The time axes allow for two complete rotations of the trapped cell. The corresponding right panels show differential interference contrast images of the RBC stained with a dye 4',6-diamidino-2-phenylindole (DAPI) that highlights the malarial parasite.

the PD voltage increasing as the malarial stage progresses, indicating stage-dependent change in the infected RBC's intrinsic birefringence. In the early stages of infection (5 h), the peak-to-peak voltage is 20 mV; this almost doubles 11 h post-infection, with a corresponding Δn change of 1.9×10^{-2} . At these times, RBC shapes are not significantly altered²⁶ and the contributions are mainly from intrinsic changes. Twenty hours postinfection, when shape changes are considerable, $\Delta n = 3 \times 10^{-2}$. Even though we follow a simplistic approach, we observe that our values of change in birefringence are not inconsistent with the one that we deduced from an earlier report based on tomographic phase microscopy of malaria-infected RBCs¹⁶ in which refractive index mapping was carried out.

It is a noteworthy feature of our results that there is a difference in the rotation observed in osmolarity-perturbed and

malaria-infected cells; the differences become marked in the latter stages of malarial infection. However, even at the early stage of infection (5 h postinfection), there are significant differences: the rotational frequency observed with osmolarity-perturbed cells is more than a factor of two different from that obtained with malaria-infected cells (5 h postinfection), at the same value of incident laser power. In the case of osmolarity-perturbed cells, the periodic rotations are fairly symmetric, whereas for malaria-infected cells, they are asymmetric 5 h postinfection. The asymmetry in the rotational data for RBCs 11 h postinfection (Fig. 4) is distinctly more marked, and we note that there is also an increase in the amplitude of rotations in comparison with the rotations obtained with osmolarity-perturbed cells. The asymmetry in the voltage value within a single cycle of rotation in the case of infected RBCs indicates that although there is an inherent ellipticity in both infected and osmolarity-altered cells, it is much more in the former case than in the latter. This becomes more apparent as the infection progresses.

Figure 5(a) shows change in retardance as a function of infection stage for different laser powers. As the infection progresses, the retardance also increases, highlighting the additional contribution to birefringence made by the parasite within the cell that gives rise to increased hemin concentration. We have already noted that upon infection by a malarial parasite, the content of hemoglobin in an RBC increases substantially, giving rise to changes in the cell's birefringence. As the malarial infection takes root (as the parasite grows over a period of 48 h), it crystallizes hemoglobin in the infected cell into hemozoin.^{12,13} We carried out separate measurements on a synthetic analog of hemozoin, hemin. We used a 10 μ l solution of hemin (dissolved in NaOH) in the same experimental setup (at varying concentrations) and we confirmed that retardance was caused [see the inset of Fig. 5(a)]. At incident laser power of 18 mW and hemin concentration of 120 mg/ml, we measured the retardance to be 10 deg. This value corresponds to retardance that we observed in RBCs 36 h postinfection.

We also found that the percentage of RBCs that rotate becomes small at higher stages of infection, as indicated by data in Fig. 5(b). This is due to increasing rigidity of the cell membrane as the infection proceeds; such increase in rigidity has been noted (and quantified) in earlier experiments in our laboratory.²⁶

Does laser light affect our measurements? We used different laser powers to confirm that our results were power-independent. Figure 5(c) show results for various infection stages. Even in case of osmolarity-perturbed cells, we did not see any change in angle with laser power. As has been described in earlier work with optical traps, our laser wavelength (1064 nm) is far removed from any absorption bands in RBCs and, consequently, we expect there to be no laser-induced photochemical reactions induced in any trapped RBC.³²

To summarize, we have studied birefringence in normal and malaria-infected red blood cells by analyzing the polarization properties of light transmitted through an optically trapped single cell. Experiments were conducted on cells whose shape was distorted by means of osmolarity alterations, giving rise to form-birefringence, which depends on cell shape and, also, on cells in which a malarial parasite was inserted, thereby inducing intrinsic birefringence. The two types of birefringence were clearly demarcated, and we succeeded in quantifying the change in refractive index for both types of cells. Malarial infections induced changes in the cell's refractive index in stage-specific fashion; these were quantitatively monitored and found to be

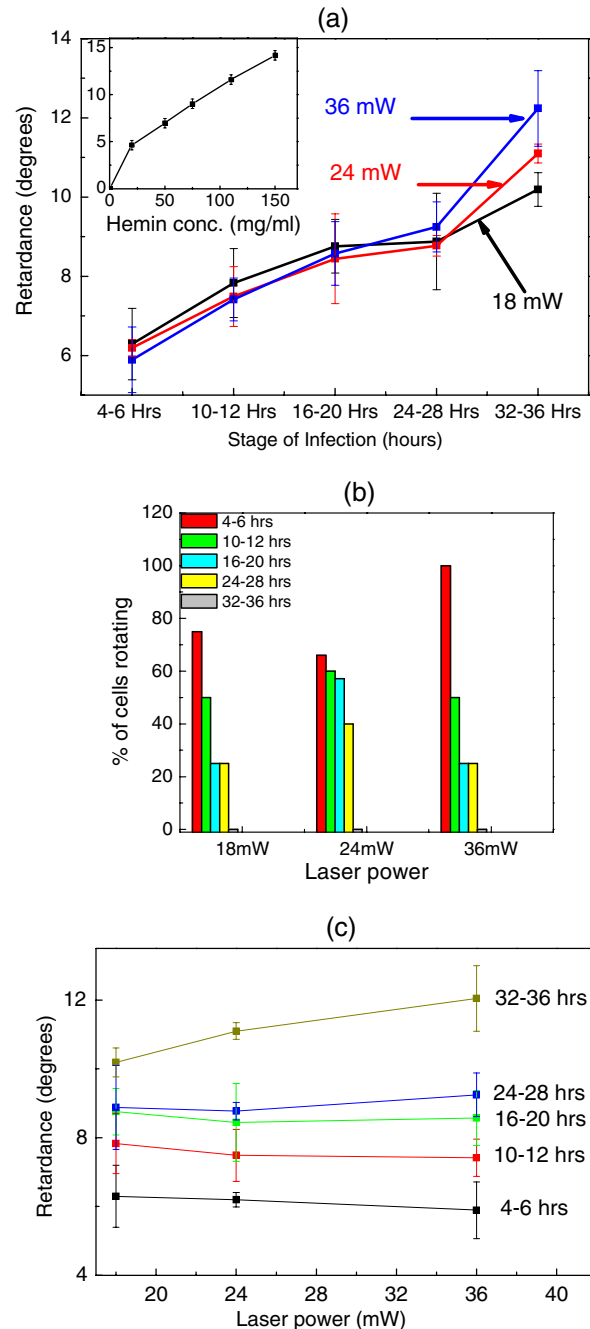


Fig. 5 (a) Retardation of the light that is induced by infected RBCs at various laser power levels. The inset shows retardation of light as it passes through a hemin solution at different concentrations. (b) Percentage of cells that rotate at various stages of infection. (c) Retardation of the light as a function of laser power. The error bars denote rms deviation.

large, in the range of 1.2 to 3×10^{-2} . Our results establish that the observed rotation of a malaria-infected RBC in an optical trap is not merely a function of shape distortion: the internal presence of the parasite also influences the rotational dynamics because of the birefringence that is induced in the RBC upon parasite infection. The degree of birefringence changes as the parasite develops inside the RBC. Our measurements have shed new light on the competition between shape- and form-birefringence in RBCs. The observed birefringence is attributed mainly to the presence of birefringent hemozoin crystals.

However, we note that early changes in birefringence at 11 h postinfection (ring stage), when very little hemozoin is present,³³ indicate the existence of additional, hitherto-unidentified factors. In *P. falciparum*, the lethal malaria species, only the ring stages occur in peripheral blood; more mature stages with high hemozoin remain sequestered to the capillaries. Thus, we demonstrate the possibility of using birefringence to establish early stages of infected parasites and of assessing various factors that contribute to birefringence in normal and infected cells. Information from our trap-based experiments may stimulate theoretical and computational efforts that have a bearing on how RBC parameters affect hematological disorders.

Acknowledgments

J. A. D. thanks the Department of Science and Technology for assistance under the Women Scientists Scheme while D. M. acknowledges generous support as a J. C. Bose National Fellow.

References

1. M. S. Valiathan, *The Legacy of Caraka*, Orient Longman, New Delhi (2003).
2. S. I. Haddad and A. A. Khairallah, "A forgotten chapter in the history of the circulation of blood," *Ann. Surg.* **104**(1), 1–8 (1936).
3. M. Meyerhof, "Ibn An-Naf's (XIIIth Cent.) and his theory of the lesser circulation," *Ibis* **23**(1), 100–120 (1935).
4. S. I. Hajdu, "A note from history: the discovery of blood cells," *Ann. Clin. Lab. Sci.* **33**(2), 237–238 (2003).
5. F. E. Cox, "History of the discovery of the malaria parasites and their vectors," *Parasit. Vectors* **3**(1), 5 (2010).
6. S. K. Mohanty and P. K. Gupta, "Optical micromanipulation methods for controlled rotation transportation and microinjection of biological objects," in *Laser Manipulation of Cells and Tissues*, M. W. Berns and K. O. Greulich, Eds., pp. 563–599, Academic Press, San Diego (2007).
7. W. Choi et al., "Tomographic phase microscopy," *Nat. Methods* **4**(9), 717–719 (2007).
8. G. Philips, S. L. Jacques, and O. J. T. McCarty, "Measurement of single cell refractive index, dry mass, volume, and density using a transillumination microscope," *Phys. Rev. Lett.* **109**(11), 118105 (2012).
9. E. Ponder and D. Barreto, "The birefringence of the human red cell ghosts," *J. Gen. Physiol.* **39**(3), 319–324 (1956).
10. J. Hofrichter, "An analysis of the birefringence intensity from gels of hemoglobin S," *J. Mol. Biol.* **96**(11), 254–256 (1975).
11. J. M. Mitchison, "Thickness and structure of the membrane of human red cell ghost," *Nature* **166**, 347–348 (1950).
12. C. Coban et al., "The malarial metabolite hemozoin and its potential use as a vaccine adjuvant," *Allergol. Int.* **59**(2), 115–124 (2010).
13. C. Romagosa et al., "Polarisation microscopy increases the sensitivity of hemozoin and Plasmodium detection in the histological assessment of placental malaria," *Acta. Trop.* **90**(3), 277–284 (2004).
14. C. Lawrence and J. A. Olson, "Birefringent hemozoin identifies malaria," *Am. J. Clin. Path.* **86**(5), 360–363 (1986).
15. M. M. Padial et al., "Sensitivity of laser light depolarization analysis for detection of malaria in blood samples," *J. Med. Microbiol.* **54**(5), 449–452 (2005).
16. Y. Park et al., "Refractive index maps and membrane dynamics of human red blood cells parasitized by Plasmodium falciparum," *Proc. Natl. Acad. Sci. U. S. A.* **105**(37), 13730–13735 (2008).
17. A. Ashkin, J. M. Dziedzic, and T. Yamane, "Optical trapping and manipulation of single cells using infrared laser beams," *Nature* **330**(6150), 769–771 (1987).
18. J. A. Dharmadhikari and D. Mathur, "Using an optical trap to fold and align single red blood cells," *Curr. Sci.* **86**(10), 1432–1437 (2004).
19. J. A. Dharmadhikari et al., "A naturally-occurring, optically-driven, cellular motor," *Appl. Phys. Lett.* **85**(24), 6048–6050 (2004).
20. S. Roy et al., "Plasmodium-infected red blood cells exhibit enhanced rolling independent of host cells and later flow of uninfected red cells," *Curr. Sci.* **89**(9), 1563–1570 (2005).
21. S. Roy et al., "Study of *P. falciparum* infected erythrocytes and induced anisotropies under optical and fluid forces," *J. Vector Borne Dis.* **44**, 23–32 (2007).
22. B. Gutiérrez-Medina et al., "An optical apparatus for rotation and trapping," *Methods Enzymol.* **475**(6), 377–404 (2010).
23. S. Parkin et al., "Optical torque on microscopic objects," *Methods Cell Biol.* **82**, 525–561 (2007).
24. J. A. Dharmadhikari et al., "Torque-generating malaria-infected red blood cells in an optical trap," *Opt. Express* **12**(6), 1179–1184 (2004).
25. A. Ghosh et al., "Euler buckling-induced folding and rotation of red blood cells in an optical trap," *Phys. Biol.* **3**(1), 67–73 (2006).
26. K. Bambardekar et al., "Shape anisotropy induces rotations in optically trapped red blood cells," *J. Biomed. Opt.* **15**(4), 041504 (2010).
27. P. Kumari et al., "Optical trapping in an absorbing medium: from optical tweezing to thermal tweezing," *Opt. Express* **20**(4), 4645–4652 (2012).
28. J. B. Jensen and W. Trager, "*P. falciparum* in culture: use of outdated erythrocytes and description of the candle jar method," *J. Parasitol.* **63**(5), 883–886 (1977).
29. C. Lambros and J. P. Vanderberg, "Synchronization of Plasmodium falciparum erythrocytic stages in culture," *J. Parasitol.* **65**(3), 418–420 (1979).
30. H. Basu et al., "Tank treading of optically-trapped red blood cells in shear flow," *Biophys. J.* **101**(7), 1604–1612 (2011).
31. E. Hecht, *Optics*, 4th ed., Addison-Wesley, New York (2002).
32. A. Bankapur et al., "Raman tweezers spectroscopy of live, single red and white blood cells," *PLoS ONE* **5**(4), e10427 (2010).
33. L. H. Bannister et al., "A brief illustrated guide to the ultrastructure of Plasmodium falciparum asexual blood stages," *Parasitol. Today* **16**(10), 427–433 (2000).